Peng Gao; Heping Dong; Fuming Ma

Inverse scattering via nonlinear integral equations method for a sound-soft crack with phaseless data

Applications of Mathematics, Vol. 63 (2018), No. 2, 149–165

Persistent URL: http://dml.cz/dmlcz/147187

63 (2018) APPLICATIONS OF MATHEMATICS No. 2, 149–165

INVERSE SCATTERING VIA NONLINEAR INTEGRAL EQUATIONS METHOD FOR A SOUND-SOFT CRACK WITH PHASELESS DATA

Peng Gao, Heping Dong, Fuming Ma, Changchun

Received June 14, 2017. First published April 8, 2018.

Abstract. We consider the inverse scattering of time-harmonic plane waves to reconstruct the shape of a sound-soft crack from a knowledge of the given incident field and the phaseless data, and we check the invariance of far field data with respect to translation of the crack. We present a numerical method that is based on a system of nonlinear and ill-posed integral equations, and our scheme is easy and simple to implement. The numerical implementation is described and numerical examples are presented to illustrate the feasibility of the proposed method.

Keywords: inverse scattering problem; Helmholtz equation; crack; phaseless; translation invariance

MSC 2010: 35R30, 78A46, 65R32, 35J05

1. Introduction

The inverse scattering problem (ISP) for cracks has numerous applications such as non-destructive testing, oil exploration, seismology and others. The inverse problem is to recover the crack from a knowledge of the incident field and the scattered time-harmonic wave at large distance, i.e., the far-field pattern. Many numerical algorithms have been suggested for the phased reconstruction problems. However, in practical applications, it is expensive and difficult to acquire the phased data of the scattered field, while obtaining the phaseless data is much easier. This motivates the phaseless inverse scattering problems and attracts more attention from both mathematics and physics. Nonetheless, the phaseless reconstruction is much more ill-posed than phased reconstruction, so it is more difficult to solve the phaseless problem. In

The research has been supported by the National Science Foundation of China (Grant No. 11371172, 11771180).

DOI: 10.21136/AM.2018.0154-17

this paper, we address the inverse scattering problem to recover a sound-soft crack from the knowledge of the incident field and the modulus of the far field pattern.

The inverse scattering problem for cracks was investigated by Kress [12] for the first time; in particular, Kress considered the inverse scattering problem for a sound-soft crack and used Newton iterations to reconstruct the crack. The case of the sound-hard crack was extended by Mönch [17]. The reconstructions acquired by this method are usually very accurate, whereas, for every iteration step, one needs to compute the solution of the forward scattering problem. Kirsch and Ritter suggested the linear sampling method [10] with the advantage that they are able to reconstruct obstacles without a priori information. A hybrid method [14] was proposed by Kress and Serranho, and it can be considered as a hybrid between a regularized Newton method and a decomposition method. In [6], Ivanyshyn and Kress extended a Newton-type method and their approach was based on some nonlinear and ill-posed integral equations for the unknown curve.

Some previous work has been done on the phaseless problems for inverse scattering, Kress and Rundell [13] investigated the two-dimensional sound-soft obstacle reconstruction from the modulus of the far-field data corresponding to a single incident plane wave. Ivanyshyn and Kress proposed the nonlinear integral equation method to reconstruct the two-dimensional sound-soft obstacles with the phaseless data in [4] and the three-dimensional sound-soft obstacles in [7]; this method involves full linearization of the integral equations system. Lee [15] presented a simple hybrid method to reconstruct the shape of the obstacle with the modulus of the far field data. Karageorghis and Johansson and Lesnic [9] proposed the method of fundamental solutions for the identification of a sound-soft obstacle with phaseless data. Ammari, Tin and Zou [1] investigated the phased and phaseless reconstructions in the inverse scattering problem via condition numbers and proved the validity of the method by numerical experiments. Bao and Zhang [2] considered the problem of reconstructing the shape of multi-scale rough surfaces from phaseless measurements. Liu and Zhang [16] gave the uniqueness result for a sound-soft ball with phaseless far field data. However, to our best knowledge, there is little study of the inverse scattering problem for the crack with phaseless data. The purpose of this paper is to reconstruct the shape of the crack with only the modulus of the far field pattern as data.

The paper is organized as follows. In Section 2, we present the inverse scattering problem with phaseless data and analyse its uniqueness with checking the invariance of far field data under translation of the crack. In Section 3, we propose our method to solve the inverse scattering problem for the sound-soft crack with phaseless data, and present the contrast between our method and the Newton method with full linearization. In Section 4, we describe the numerical implementation of the iterative

scheme in detail and present some numerical examples to illustrate the feasibility of our method.

2. Inverse scattering problem with phaseless data and its uniqueness

Let us describe the inverse scattering problem for cracks in its mathematical formulation. Assume that $\Gamma_c \subset \mathbb{R}^2$ is a crack of class $\mathcal{C}^3$, i.e.

$$\Gamma_c = \{z(s)\colon\ s \in [-1,1]\},$$

where $z\colon [-1,1] \to \mathbb{R}^2$ is injective and $\mathcal{C}^3$ smooth, $|z'(s)| \neq 0$ for all s. Given an incident plane wave $u^i(x) = \mathrm{e}^{\mathrm{i}kx\cdot d}$, $x \in \mathbb{R}^2$ with wave number $k > 0$ and the direction of propagation d, the direct scattering problem for a sound-soft crack is to find the total field $u = u^i + u^s$ as a solution to the Helmholtz equation

$$\Delta u + k^2 u = 0 \quad \text{in } \mathbb{R}^2 \setminus \Gamma_c \tag{2.1}$$

with the Dirichlet boundary condition

$$u = 0 \quad \text{on } \Gamma_c, \tag{2.2}$$

such that the unknown scattered wave u^s satisfies the Sommerfeld radiation condition

$$\lim_{r\to\infty} \sqrt{r}\Big(\frac{\partial u^s}{\partial r} - \mathrm{i}ku^s\Big) = 0, \quad r = |x|, \tag{2.3}$$

uniformly with respect to all directions. The radiation condition (2.3) ensures an asymptotic behaviour of the form

$$u^s(x) = \frac{\mathrm{e}^{\mathrm{i}k|x|}}{\sqrt{|x|}}\Big\{u_\infty(\hat{x}) + O\Big(\frac{1}{|x|}\Big)\Big\}, \quad |x| \to \infty$$

uniformly in all directions $\hat{x} = x/|x|$, and the far-field pattern u_∞ of the scattered wave u^s is defined on the unit circle $\Omega \subset \mathbb{R}^2$.

(ISP). The corresponding inverse scattering problem we are concerned with is to determine the shape of the sound-soft crack Γ_c with the given $|u_\infty|$ which is the modulus of the far field pattern for one incident plane wave u^i.

For the scattering problem, by the Huygens principle ([3], Theorem 3.14), we have

$$u(x) = u^i(x) - \int_{\Gamma_c} \Phi(x,y)\varphi(y)\,\mathrm{d}s(y), \quad x \in \mathbb{R}^2 \setminus \Gamma_c, \tag{2.4}$$

in terms of the fundamental solution to the Helmholtz equation

$$\Phi(x,y) = \frac{\mathrm{i}}{4} H_0^{(1)}(k|x-y|), \quad x \neq y,$$

where $H_0^{(1)}$ denotes the Hankel function of the first kind and order zero. To take care of the singularities at the end points of the crack, from [12] we know that the density φ is assumed to be

$$\varphi(x) = \frac{\widetilde{\varphi}(x)}{\sqrt{|x-z_1||x-z_{-1}|}}, \quad x \in \Gamma_{\mathrm{c}} \setminus \{z_1, z_{-1}\},$$

where $\widetilde{\varphi}(x) \in C(\Gamma_{\mathrm{c}})$, $z_1 := z(1)$ and $z_{-1} := z(-1)$ are the end points of Γ_{c}. The far field pattern of the scattered field u^s is in the form of

$$u_\infty(\hat{x}) = \gamma \int_{\Gamma_{\mathrm{c}}} \mathrm{e}^{-\mathrm{i}k\hat{x}\cdot y} \varphi(y)\, \mathrm{d}s(y), \quad \hat{x} \in \Omega, \tag{2.5}$$

where $\gamma = \mathrm{e}^{\mathrm{i}\pi/4}/\sqrt{8k\pi}$. We introduce the single-layer operator $S_c\colon\ L^p(\Gamma_{\mathrm{c}}) \to C(\Gamma_{\mathrm{c}})$, $1 < p < \infty$,

$$(S_c\varphi)(x) = \int_{\Gamma_{\mathrm{c}}} \Phi(x,y)\varphi(y)\, \mathrm{d}s(y), \quad x \in \Gamma_{\mathrm{c}}.$$

The operator S_c is linear and bounded. The far field operator $S_{c,\infty}\colon\ L^p(\Gamma_{\mathrm{c}}) \to L^2(\Omega)$ is defined by

$$(S_{c,\infty}\varphi)(x) = \gamma \int_{\Gamma_{\mathrm{c}}} \mathrm{e}^{-\mathrm{i}k\hat{x}\cdot y} \varphi(y)\, \mathrm{d}s(y), \quad \hat{x} \in \Omega.$$

From (2.4) and (2.5), we can observe that the unknown curve Γ_{c} and density φ satisfy the equations

$$S_c\varphi = u^i|_{\Gamma_{\mathrm{c}}}, \tag{2.6}$$

$$|S_{c,\infty}\varphi|^2 = |u_\infty|^2. \tag{2.7}$$

The equation (2.6) ensures that the boundary condition is $u = 0$ on Γ_{c}, and equation (2.7) implies that the scattered field u^s given by (2.4) has the correct modulus of the far field pattern.

The uniqueness of the inverse scattering problem for the sound-soft crack with one incident plane wave was investigated in [11], it was proposed that the far field pattern for one incident plane wave uniquely determines Γ_{c} if the unknown crack Γ_{c} is contained in the disk of radius R such that $kR \leqslant \lambda_0$, where λ_0 denotes the smallest zero of the Bessel function J_0. For the problem of inverse obstacle scattering with phaseless data, Kress and Rundell gave the translation invariance in [13]; it

implies that the solution to the inverse scattering problem is not unique, therefore, we cannot recover the location of the obstacle from the modulus of the far field pattern. Analogously to [13], we present the following result.

Theorem 1. *Assume that $u_\infty(\hat{x})$ is the far field pattern of scattering from a sound-soft crack Γ_c. Then, for the cracks $\Gamma_c^\varepsilon := \{x + \varepsilon h\colon\ x \in \Gamma_c\}$ with $h \in \mathbb{R}^2$, the far field pattern u_∞^ε have the form*

$$u_\infty^\varepsilon(\hat{x}) = \mathrm{e}^{\mathrm{i}k\varepsilon h\cdot(d-\hat{x})} u_\infty(\hat{x}), \quad \hat{x} \in \Omega, \tag{2.8}$$

that is, the inverse scattering problem for the sound-soft crack with the modulus of the far field pattern has the translation invariance.

P r o o f. By using equations (2.6) and (2.7), we obtain

$$\int_{\Gamma_c^\varepsilon} \Phi(x,y)\varphi_\varepsilon(y)\,\mathrm{d}s(y) = u^i(x), \quad x \in \Gamma_c^\varepsilon. \tag{2.9}$$

If $\varphi(y)$ is the solution of (2.6), then we obtain that $\varphi_\varepsilon(x) = \mathrm{e}^{\mathrm{i}k\varepsilon h\cdot d}\varphi(x-\varepsilon h)$, $x \in \Gamma_c^\varepsilon$, is the solution of (2.9). In fact, we substitute it to the left-hand side of equation (2.9),

$$\begin{aligned}\int_{\Gamma_c^\varepsilon} \Phi(x,y)\varphi_\varepsilon(y)\,\mathrm{d}s(y) &= \int_{\Gamma_c^\varepsilon} \Phi(x,y)\mathrm{e}^{\mathrm{i}k\varepsilon h\cdot d}\varphi(y-\varepsilon h)\,\mathrm{d}s(y)\\ &= \int_{\Gamma_c} \Phi(\tilde{x},\tilde{y})\mathrm{e}^{\mathrm{i}k\varepsilon h\cdot d}\varphi(\tilde{y})\,\mathrm{d}s(\tilde{y}) = \mathrm{e}^{\mathrm{i}k\varepsilon h\cdot d}u^i(\tilde{x}) = u^i(x),\end{aligned}$$

where $\tilde{x} = x - \varepsilon h$ and $\tilde{y} = y - \varepsilon h$. Then the far field on Γ_c^ε is

$$\begin{aligned}u_\infty^\varepsilon(\hat{x}) &= \gamma \int_{\Gamma_c^\varepsilon} \mathrm{e}^{-\mathrm{i}k\hat{x}\cdot y}\varphi_\varepsilon(y)\,\mathrm{d}s(y) = \gamma \int_{\Gamma_c^\varepsilon} \mathrm{e}^{-\mathrm{i}k\hat{x}\cdot y}\mathrm{e}^{\mathrm{i}k\varepsilon h\cdot d}\varphi(y-\varepsilon h)\,\mathrm{d}s(y)\\ &= \gamma \int_{\Gamma_c} \mathrm{e}^{-\mathrm{i}k\hat{x}\cdot y}\mathrm{e}^{\mathrm{i}k\varepsilon h\cdot d}\varphi(\tilde{y})\,\mathrm{d}s(\tilde{y}) = \mathrm{e}^{\mathrm{i}k\varepsilon h\cdot(d-\hat{x})}u_\infty(\hat{x}),\end{aligned}$$

so (2.8) is proved. Obviously, we obtain $|u_\infty^\varepsilon(\hat{x})| = |u_\infty(\hat{x})|$, so the modulus of the far field pattern $|u_\infty|$ is invariant under translation. The proof is completed. □

Due to the translation invariance, we cannot recover the location of the sound-soft crack for one incident plane wave with the modulus of the far field pattern as the data.

3. Iterative scheme

Let us consider the method of solving inverse scattering problem numerically. We suggest an iterative method to solve the system of nonlinear integral equations (2.6), (2.7) and make an approximation to Γ_c.

To deal with the singularities of the density φ, we use the cosine transformation as suggested by Yan and Sloan [18]. We substitute $s = \cos t$, $t \in [0, \pi]$, into the parametric representation of Γ_c, with $x(t) := z(\cos t)$, $y(\tau) := z(\cos \tau)$, where $0 \leqslant t$, $\tau \leqslant \pi$, and transform the integral operator S_c into the parameterized operator C, given by

$$C(z,\psi)(t) = \frac{\mathrm{i}}{4} \int_0^\pi H_0^1(k|z(\cos t) - z(\cos \tau)|)\psi(\tau)\,\mathrm{d}\tau, \quad t \in [0,\pi], \tag{3.1}$$

where

$$\psi(t) := |\sin t|\,|z'(\cos t)|\varphi(z(\cos t)), \quad t \in [0,\pi].$$

Analogously, we introduce the parameterized the far field operator C_∞:

$$C_\infty(z,\psi)(t) = \gamma \int_0^\pi \mathrm{e}^{-\mathrm{i}kz_\infty(t)\cdot z(\tau)}\psi(\tau)\,\mathrm{d}\tau, \quad t \in [0,2\pi], \tag{3.2}$$

where

$$z_\infty(t) = (\cos t, \sin t), \quad t \in [0,2\pi].$$

In addition, we parameterize the incident field u^i and the far field pattern u_∞ by the form of $\omega_c = u^i \circ z$ and $|\omega_{c,\infty}| = |u_\infty| \circ z_\infty$. Using this notation, the parametric form of equations (2.6)–(2.7) is given by

$$C(z,\psi) = \omega_c(z), \tag{3.3}$$

$$\overline{C_\infty(z,\psi)}C_\infty(z,\psi) = |\omega_{c,\infty}|^2. \tag{3.4}$$

The Fréchet derivative of $C_\infty(z,\psi)$ with respect to z has the representation

$$C'_\infty[z,\psi]q = -\mathrm{i}k\gamma \int_0^\pi \mathrm{e}^{-\mathrm{i}kz_\infty(t)\cdot z(\tau)} z_\infty(t) q(\tau)\psi(\tau)\,\mathrm{d}\tau \quad \forall\, q \in C^2[0,\pi] \times C^2[0,\pi]. \tag{3.5}$$

Therefore, the derivative of $\overline{C_\infty}C_\infty$ with respect to z is given by

$$(\overline{C_\infty(z,\psi)}C_\infty(z,\psi))'q = 2\Re(\overline{C_\infty(z,\psi)}C'_\infty[z,\psi]q) \quad \forall\, q \in C^2[0,\pi] \times C^2[0,\pi].$$

The linearization of (3.4) leads to

$$B[z,\psi]q = f^{z,\psi}, \tag{3.6}$$

where $B[z,\psi]q := 2\Re(\overline{C_\infty(z,\psi)}C'_\infty[z,\psi]q)$ and $f^{z,\psi} := |\omega_{c,\infty}|^2 - |C_\infty(z,\psi)|^2$.

The suggested iterative procedure is the following:

(1) Make an initial guess for the curve Γ_c and find the density ψ from (3.3).

(2) The equation (3.6) needs to be solved for q to obtain the update $z+q$ for the curve approximation.
(3) The procedure continues by repeating the previous two steps until a suitable stopping criterion is satisfied.

The stopping criterion for the iterative procedure is in the form of

$$E_k := \frac{\||w_{c,\infty}|^2 - |C_\infty(z,\psi)|^2\|_{L^2}}{\||w_{c,\infty}|^2\|_{L^2}} \leqslant \varepsilon \tag{3.7}$$

for some sufficiently small tolerance $\varepsilon > 0$ which depends on the noise level of data.

Let us denote

$$A[z,\psi] = \frac{\partial(\overline{C_\infty(z,\psi)}C_\infty(z,\psi))}{\partial\psi},$$

and $q = z_{k+1} - z_k$, $p = \psi_{k+1} - \psi_k$. The operator $C(z,\psi)$ is linear on ψ, so we denote it as $C(z)\psi$. In the Newton method, we have to solve the following equations in each iterative step:

$$\begin{bmatrix} C'(z_k)\psi_k - \omega_c'(z_k) & C(z_k) \\ B[z_k,\psi_k] & A[z_k,\psi_k] \end{bmatrix} \begin{bmatrix} q \\ p \end{bmatrix} = \begin{bmatrix} \omega_c(z_k) - C(z_k)\psi_k \\ |\omega_{c,\infty}|^2 - |C_\infty(z_k,\psi_k)|^2 \end{bmatrix}. \tag{3.8}$$

However, the iteration scheme of our method we suggested in this paper is to solve equations

$$\begin{bmatrix} B[z_k,\psi_{k+1}] & 0 \\ 0 & C(z_k) \end{bmatrix} \begin{bmatrix} q \\ p \end{bmatrix} = \begin{bmatrix} |\omega_{c,\infty}|^2 - |C_\infty(z_k,\psi_{k+1})|^2 \\ \omega_c(z_k) - C(z_k)\psi_k \end{bmatrix} \tag{3.9}$$

as in reference [8]. Our iterative procedure is little different from the Newton method to solve equations (3.3) and (3.4). To solve (3.9), we need only to solve two independent equations. It is easy to see that our scheme can be easily realized and reduces the computational cost.

4. Numerical implementation and numerical examples

4.1. Numerical implementation. In this section, we describe how to numerically solve the equation (3.3) and (3.6) in our algorithm.

For equation (3.3), with fixed z, we solve an integral equation of the form

$$\frac{\mathrm{i}}{4}\int_0^\pi H_0^{(1)}(k|z(\cos t) - z(\cos\tau)|)\psi(\tau)\,\mathrm{d}\tau = \omega_c(t), \quad t \in [0,\pi], \tag{4.1}$$

for the unknown function $\psi(\tau)$ by using Nyström method in [12], where

$$\psi(t) := |\sin t||z'(\cos t)|\varphi(z(\cos t)). \tag{4.2}$$

For the following analysis, it is more convenient to transform the integral equation to an equation over the interval $[0, 2\pi]$ than $[0, \pi]$. The solution $\psi \in C[0, \pi]$ in the form of (4.2) for the integral equation (4.1) is equivalent to an even 2π-periodic solution ψ of the integral equation

$$\frac{1}{2\pi}\int_0^{2\pi} K(t,\tau)\psi(\tau)\,\mathrm{d}\tau = f(t), \quad 0 \leqslant t \leqslant 2\pi, \tag{4.3}$$

where the kernel is

$$K(t,\tau) := \frac{\pi}{2\mathrm{i}} H_0^{(1)}(k|z(\cos t) - z(\cos\tau)|), \quad t \neq \tau,$$

and

$$f(t) := -2u^i(z(\cos t)).$$

Noting that we can split the kernel K into the form

$$K(t,\tau) = \Big\{1 + \sin^2\frac{t-\tau}{2} K_1(t,\tau)\Big\} \ln\Big(\frac{4}{\mathrm{e}}\sin^2\frac{t-\tau}{2}\Big) + K_2(t,\tau),$$

by the quadrature rules, we obtain the linear system

$$\sum_{j=0}^{2n-1} \psi_n(t_j^{(n)})\Big\{R_{|k-j|}^{(n)} + P_{|k-j|}^{(n)}(t) K_1(t_k^{(n)}, t_j^{(n)}) + \frac{1}{2n} K_2(t_k^{(n)}, t_j^{(n)})\Big\} = f(t_k^{(n)}), \tag{4.4}$$
$$k = 0, \ldots, n$$

where

$$R_j^{(n)} = \frac{1}{2n}\Big\{c_0 + 2\sum_{m=1}^{n-1} c_m \cos\frac{mj\pi}{n} + (-1)^j c_n\Big\},$$

$$P_j^{(n)} = \frac{1}{2n}\Big\{\gamma_0 + 2\sum_{m=1}^{n-1} \gamma_m \cos\frac{mj\pi}{n} + (-1)^j \gamma_n\Big\}$$

and

$$c_m = -\frac{1}{\max(1, |m|)}, \quad \gamma_m = \frac{1}{4}(2c_m - c_{m+1} - c_{m-1}).$$

It is easy to see that the linear system (4.4) has $2n$ unknown nodal values of ψ_n, but it only has $n+1$ equations. To solve (4.4), we make use of the symmetry property $\psi_n(t_k^{(n)}) = \psi_n(t_{2n-k}^{(n)})$ for $k = 0, \ldots, n$, so we only need to solve a system with $n+1$ unknowns and $n+1$ equations.

Now, we discuss the discretization of the linearized equation (3.6). As a finite dimensional subspace for the reconstruction z and its update q, we choose the space spanned by the Chebyshev polynomials of the form

$$q_c(s) = \sum_{m=0}^{M} a_m T_m(s), \quad s \in [-1, 1] \tag{4.5}$$

with the coefficients $a_m \in \mathbb{R}^2$. Applying the cosine transformation, we take $q(t) = q_c(\cos t)$, also $T_m(\cos t) = \cos mt$, then we obtain the representation by the even trigonometrical polynomials

$$q(t) = \sum_{m=0}^{M} a_m \cos mt, \quad t \in [0, \pi]. \tag{4.6}$$

Setting

$$M^{z,\psi}(t,\tau) = \gamma \mathrm{e}^{-\mathrm{i}kz_\infty(t)\cdot z(\tau)}\psi(\tau)$$

and

$$N^{z,\psi}(t,\tau) = -\mathrm{i}k\gamma \mathrm{e}^{-\mathrm{i}kz_\infty(t)\cdot z(\tau)}\psi(\tau),$$

we solve the linear system of the form

$$\sum_{m=0}^{M} a_m (B[z,\psi]\cos m\tau)(t_s) = f^{z,\psi}(t_s), \quad s = 1, \dots, N, \tag{4.7}$$

to determine the real coefficients $a_m := (\alpha_m, \beta_m)$, where

$$(B[z,\psi]\chi(\tau))(t) = 2\Re\biggl\{\overline{\int_0^\pi M^{z,\psi}(t,\tau)\,\mathrm{d}\tau}\int_0^\pi N^{z,\psi}(t,\tau)z_\infty(t)\chi(\tau)\,\mathrm{d}\tau\biggr\}. \tag{4.8}$$

By using (4.7) and (4.8), we obtain the linear system

$$\begin{aligned} &2\Re\biggl\{\overline{\int_0^\pi M^{z,\psi}(t,\tau)\,\mathrm{d}\tau}\int_0^\pi N^{z,\psi}(t,\tau)\cos m\tau\,\mathrm{d}\tau\biggl(\sum_{m=0}^{M}\alpha_m\cos t + \sum_{m=0}^{M}\beta_m \sin t\biggr)\biggr\} \\ &\qquad = f^{z,\psi}(t_s). \end{aligned} \tag{4.9}$$

We rewrite the linear system (4.9) to the form

$$\sum_{m=0}^{M}\alpha_m L^{z,\psi}(t_s)\cos t_s + \sum_{m=0}^{M}\beta_m L^{z,\psi}(t_s)\sin t_s = f^{z,\psi}(t_s), \tag{4.10}$$

where

$$(L^{z,\psi}\chi(\tau))(t) = 2\Re\biggl\{\overline{\int_0^\pi M^{z,\psi}(t,\tau)\,\mathrm{d}\tau}\int_0^\pi N^{z,\psi}(t,\tau)\cos m\tau\chi(\tau)\,\mathrm{d}\tau\biggr\}. \tag{4.11}$$

To solve (4.10), regularization is necessary and we minimize the penalized defect

$$\begin{aligned} &\sum_{s=1}^{N}\biggl|\sum_{m=0}^{M}\alpha_m L^{z,\psi}(t_s)\cos t_s + \sum_{m=0}^{M}\beta_m L^{z,\psi}(t_s)\sin t_s - f^{z,\psi}(t_s)\biggr|^2 \\ &\qquad + \lambda\biggl(2\pi(\alpha_0^2+\beta_0^2) + \pi\sum_{m=1}^{M}(1+m^2)(\alpha_m^2+\beta_m^2)\biggr) \end{aligned} \tag{4.12}$$

with a positive regularization parameter λ and an H^1 penalty term. We transform (4.11) from $[0,\pi]$ to the interval $[0,2\pi]$, and, due to the trapezoidal rule, we obtain the approximation of $L_m^{z,\psi}(t_s)\cos t_s$

$$L_m^c(t_s)=\frac{1}{2}\Big(\frac{\pi}{n}\Big)^2\sum_{j=0}^{2n-1}\sum_{l=0}^{2n-1}\Re\{\overline{M^{z,\psi}(t_s,\tau_l)}N^{z,\psi}(t_s,\tau_j)\cos m\tau_j\cos t_s\}$$

and the approximation of $L_m^{z,\psi}(t_s)\sin t_s$

$$L_m^s(t_s)=\frac{1}{2}\Big(\frac{\pi}{n}\Big)^2\sum_{j=0}^{2n-1}\sum_{l=0}^{2n-1}\Re\{\overline{M^{z,\psi}(t_s,\tau_l)}N^{z,\psi}(t_s,\tau_j)\cos m\tau_j\sin t_s\}.$$

Then, the minimizer in (4.12) is observed as the unique solution of the equation

$$\lambda\tilde{I}\xi+L^*L\xi=L^*f \tag{4.13}$$

with $\tilde{I}=\operatorname{diag}\{2\pi,(1+1^2)\pi,\ \ldots,\ (1+M^2)\pi,\ 2\pi,\ (1+1^2)\pi,\ \ldots,\ (1+M^2)\pi\}$, $f=(f^{z,\psi}(t_1),\ldots,f^{z,\psi}(t_N))^{\mathrm{T}}$, $\xi=(\alpha_0,\ldots,\alpha_M,\beta_0,\ldots,\beta_M)^{\mathrm{T}}$, $L=(L_0^c,\ldots,L_M^c,$ $L_0^s,\ldots,L_M^s)$.

As for the update ξ, we obtain it from a scaled Newton step with Tikhonov regularization and H^1 penalty term,

$$\xi=\varrho(\lambda\tilde{I}+L^*L)^{-1}L^*f$$

with the scaling factor $\varrho\geqslant 0$.

4.2. Numerical examples. Based on the above, we present some numerical examples to illustrate the feasibility of the iterative reconstruction method for the sound-soft cracks case. In order to avoid committing an inverse crime, we choose different numbers of quadrature points for the forward and the inverse problem and added noises to the data. The following examples are all obtained with $n=100$ quadrature points for the forward problem and $n=50$ for the inverse problem. The noisy data $|u_\infty^\delta|^2$ is constructed in the form

$$|u_\infty^\delta|^2=|u_\infty|^2+\delta\eta\frac{\||u_\infty|^2\|_{L^2}}{\|\eta\|_{L^2}}, \tag{4.14}$$

where δ is the relative noise level and η is normally distributed random variable. As presented in [5], the regularization parameter λ in equation (4.13) can be chosen as

$$\lambda_k=\||w_{c,\infty}|^2-|C_\infty(z_{k-1},\psi_{k-1})|^2\|_{L^2}^{\mu},\quad \mu>0,\ k=1,2,\ldots$$

From Theorem 1, we have the translation invariance of the sound-soft crack with phaseless data, so that the location of the cracks cannot be determined only with

the modulus of the far field data. Based on this property, in the following numerical examples, we determine the coefficient a_0 in Chebyshev polynomials (4.6) in the iteration procedure to fix the location of the reconstructed curve. If we set different values of a_0, this leads to a shifted curve (see Figure 1). When we set a_0 to be equal to the correct value of the real curve, the reconstructed curve can be at the location of the actual curve (see Figures 2–7), it helps us to compare the reconstructed curve with the real curve in the numerical experiments.

In the numerical examples, we choose always $\mu = 1$ and use the stopping criteria (3.7). In all the figures, we denote the initial guess by dash dot line, the actual arc by solid line, the reconstructions arc by the dashed line. The arrow in the figures shows the direction of the incoming wave.

E x a m p l e 1. In the first example, we consider the reconstruction of the crack with the representation

$$z(s) = (s, s^2), \quad s \in [-1, 1]. \tag{4.15}$$

We set the wave number $k = 2$, $\varrho = 0.8$, and $M = 15$. In Figure 1, we use a half ellipse to be the initial curve and 1% noisy data; this figure shows the translation invariance of the phaseless far field data. In the following figures of the crack (4.15), we always use the 1% and 10% noisy data. For Figure 2, we use a half ellipse to be the initial guess and choose different incoming directions to reconstruct the cracks respectively. In Figure 3, we change the initial guess to be a line and also we choose the initial guess far from the actual curve. We observe that the different incoming directions can influence the effect of the reconstruction.

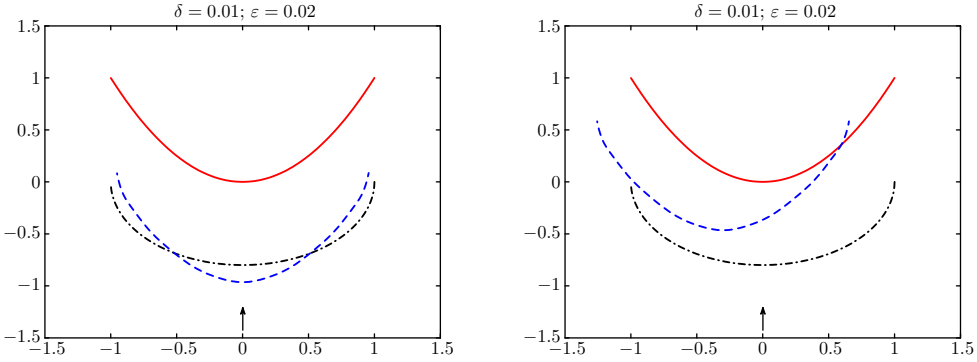

(a) (b)

Figure 1. Reconstructions (dashed line) of crack (4.15) with $d = (0, 1)$, $\delta = 1\%$ and initial guess (dash dot line): $z_0(s) = (s, -0.8\sqrt{1 - s^2})$, $s \in [-1, 1]$.

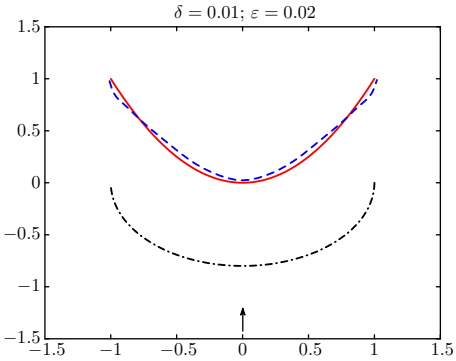

(a) $d = (0, 1)$, $\delta = 1\%$

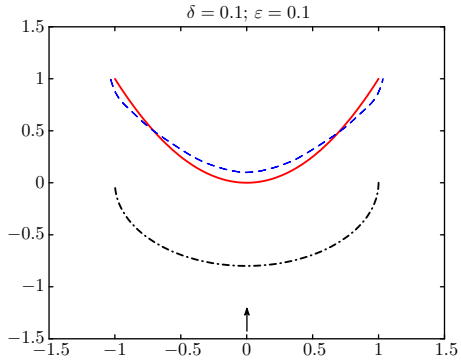

(b) $d = (0, 1)$, $\delta = 10\%$

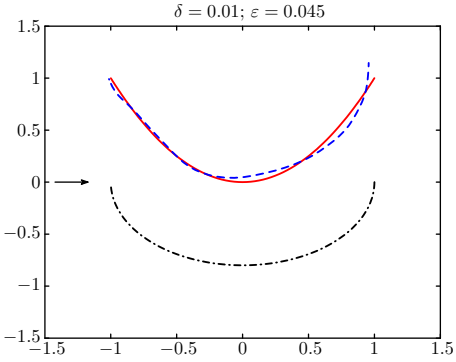

(c) $d = (1, 0)$, $\delta = 1\%$

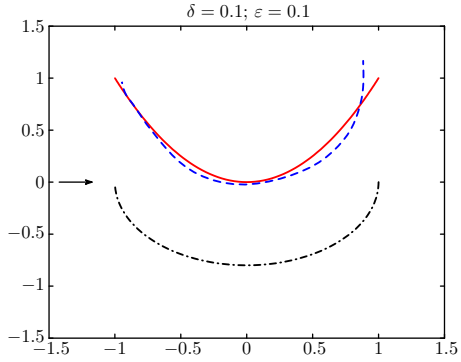

(d) $d = (1, 0)$, $\delta = 10\%$

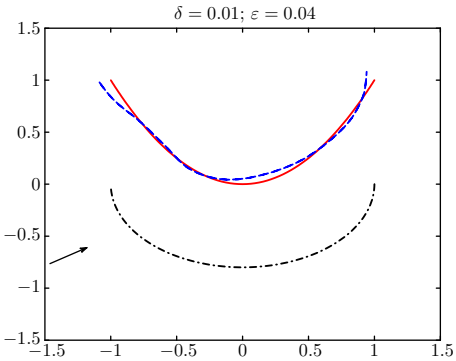

(e) $d = (\cos\frac{\pi}{6}, \sin\frac{\pi}{6})$, $\delta = 1\%$

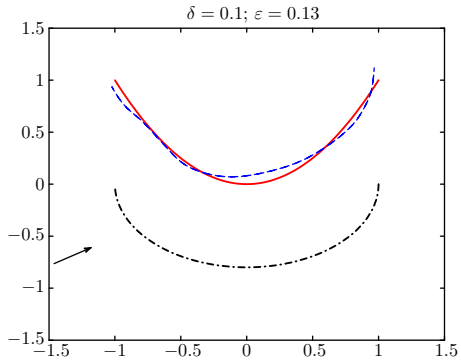

(f) $d = (\cos\frac{\pi}{6}, \sin\frac{\pi}{6})$, $\delta = 10\%$

Figure 2. Reconstructions (dashed line) of crack (4.15) with the initial guess (dash dot line): $z_0(s) = (s, -0.8\sqrt{1 - s^2})$, $s \in [-1, 1]$, different incoming directions d and different noisy level δ.

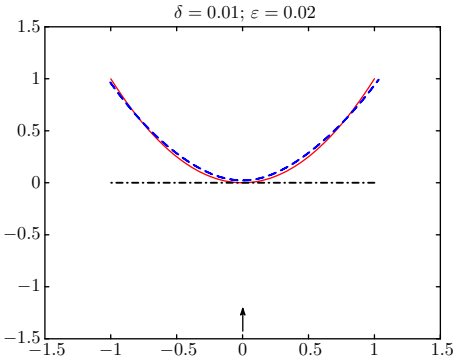

(a) $z_0(s) = (s, 0)$, $\delta = 1\%$

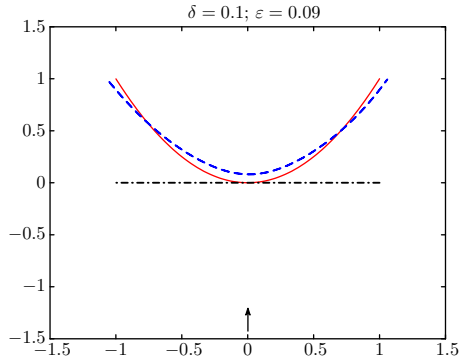

(b) $z_0(s) = (s, 0)$, $\delta = 10\%$

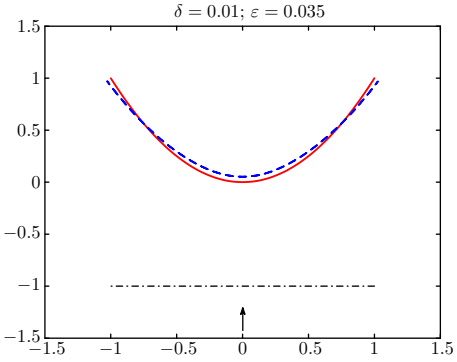

(c) $z_0(s) = (s, -1)$, $\delta = 1\%$

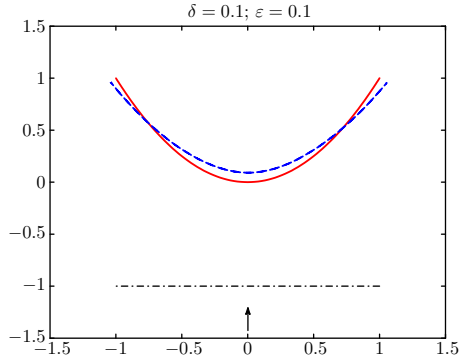

(d) $z_0(s) = (s, -1)$, $\delta = 10\%$

Figure 3. Reconstructions (dashed line) of crack (4.15) with $d = (0, 1)$, different noisy level δ, and different initial guesses (dash dot line) $z_0(s)$, $s \in [-1, 1]$.

E x a m p l e 2. For the second example, we choose a crack of the form

$$z(s) = \Big(s, 0.5\cos\frac{\pi s}{2} + 0.2\sin\frac{\pi s}{2} - 0.1\cos\frac{3\pi s}{2}\Big), \quad s \in [-1, 1]. \tag{4.16}$$

We set $\varrho = 1.1$, the wave number $k = 4$, the incoming direction $d = (1, 0)$ and $M = 15$. In the following figures of the crack (4.16), we always use the 1% and 10% noisy data to reconstruct the cracks. It can be seen from Figure 4 that we can reconstruct the crack even with the initial guess far from the exact curve. For Figure 5, we choose the initial guess of a different shape to reconstruct the curve.

E x a m p l e 3. In the last example, we present the sound-soft crack with the parametric representation

$$z(s) = \Big(2\sin\frac{s}{2}, \sin s\Big), \quad s \in \Big[\frac{\pi}{4}, \frac{7\pi}{4}\Big]. \tag{4.17}$$

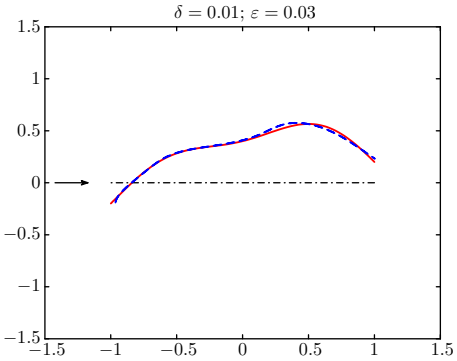

(a) $z_0(s) = (s, 0)$, $\delta = 1\%$

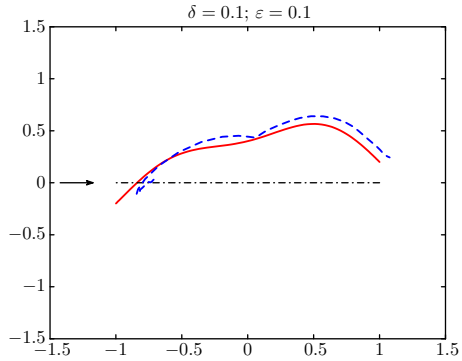

(b) $z_0(s) = (s, 0)$, $\delta = 10\%$

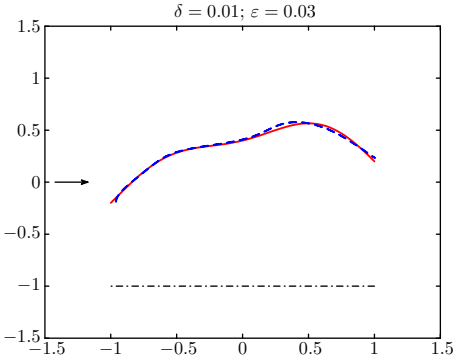

(c) $z_0(s) = (s, -1)$, $\delta = 1\%$

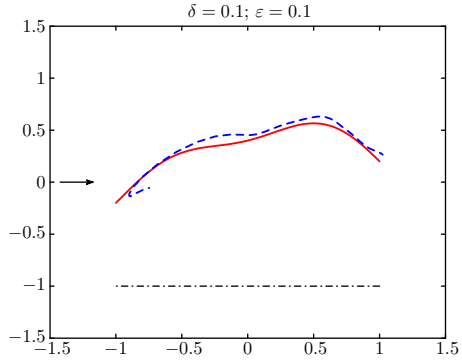

(d) $z_0(s) = (s, -1)$, $\delta = 10\%$

Figure 4. Reconstructions (dashed line) of crack (4.16) with $d = (1, 0)$, different noisy level δ, and different initial guesses (dash dot line) $z_0(s)$, $s \in [-1, 1]$.

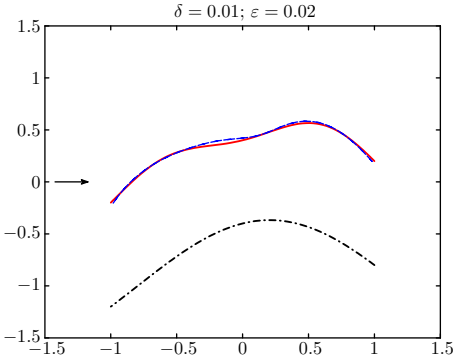

(a) $\delta = 1\%$

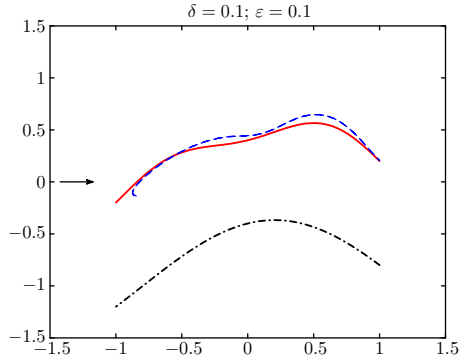

(b) $\delta = 10\%$

Figure 5. Reconstructions (dashed line) of crack (4.16) with the initial guess (dash dot line): $z_0(s) = \big(s, 0.6\cos\frac{1}{2}\pi s + 0.2\sin\frac{1}{2}\pi s - 1\big)$, $s \in [-1, 1]$, $d = (1, 0)$, and different noisy level δ.

We set the wave number $k = 3$, $M = 15$, $d = (-1, 0)$. In the following figures of the crack (4.17), we always use the 1% and 10% noisy data to reconstruct the cracks. In Figure 6, $\varrho = 0.8$, we choose different locations of the initial guess to reconstruct the curve with noisy data respectively. In Figure 7, $\varrho = 1.5$, we change the shape of the initial guess line to reconstruct the crack.

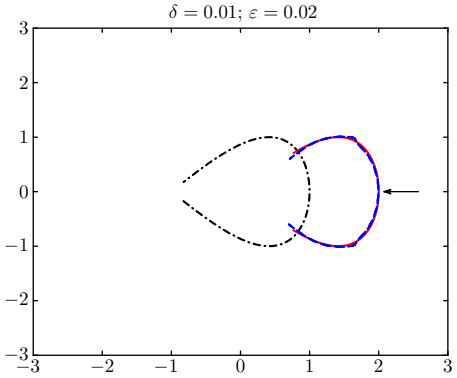

(a) $\delta = 1\%$,
$z_0(s) = \left(2\sin\left(\frac{17}{36}\pi s + \frac{1}{2}\pi\right) - 1, \sin\left(\frac{17}{18}\pi s + \pi\right)\right)$

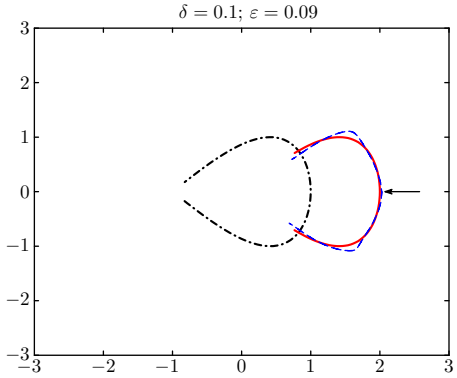

(b) $\delta = 10\%$,
$z_0(s) = \left(2\sin\left(\frac{17}{36}\pi s + \frac{1}{2}\pi\right) - 1, \sin\left(\frac{17}{18}\pi s + \pi\right)\right)$

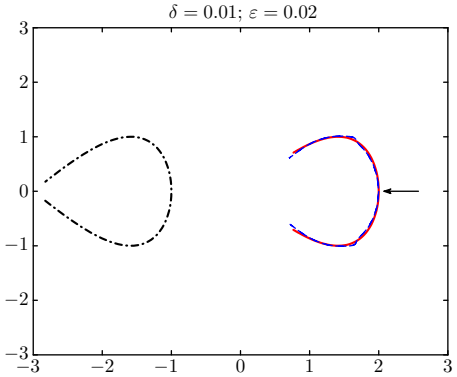

(c) $\delta = 1\%$,
$z_0(s) = \left(2\sin\left(\frac{17}{36}\pi s + \frac{1}{2}\pi\right) - 3, \sin\left(\frac{17}{18}\pi s + \pi\right)\right)$

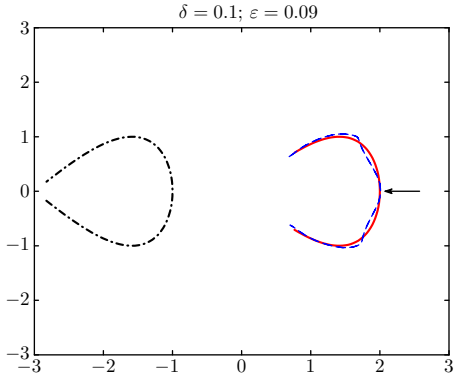

(d) $\delta = 10\%$,
$z_0(s) = \left(2\sin\left(\frac{17}{36}\pi s + \frac{1}{2}\pi\right) - 3, \sin\left(\frac{17}{18}\pi s + \pi\right)\right)$

Figure 6. Reconstructions (dashed line) of crack (4.17) with $d = (-1, 0)$, different noisy level δ, and different initial guesses (dash dot line) $z_0(s)$, $s \in [-1, 1]$.

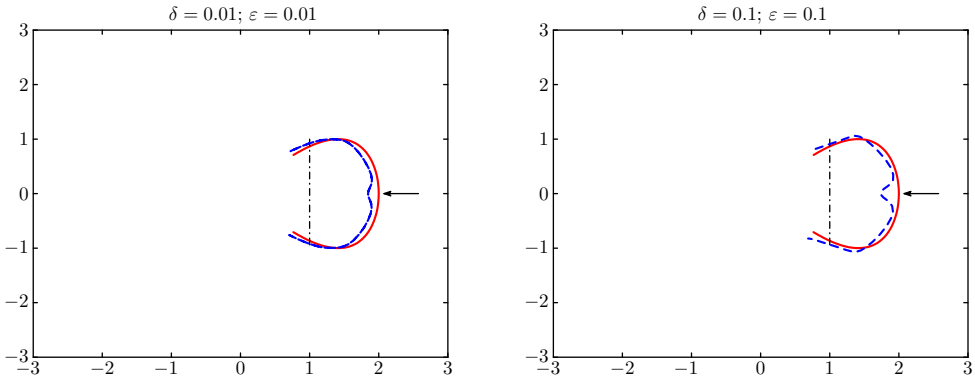

(a) $\delta = 1\%$ (b) $\delta = 10\%$

Figure 7. Reconstructions (dashed line) of crack (4.17) with the initial guess (dash dot line): $z_0(s) = (1, s)$, $s \in [-1, 1]$, $d = (-1, 0)$, and different noisy level δ.

5. Conclusions

We have proposed an iterative method to solve the inverse scattering problem for the sound-soft crack with phaseless data and check the invariance of far field data under translation of the crack. Then, we point out the difference between our method and the Newton method. Our method is easier to implement than the Newton method and reduces the computational cost. Also the numerical implementation of our iterative scheme is described, and numerical examples are presented to illustrate the feasibility of the iterative method.

References

[1] *H. Ammari, Y. T. Chow, J. Zou*: Phased and phaseless domain reconstructions in the inverse scattering problem via scattering coefficients. SIAM J. Appl. Math. *76* (2016), 1000–1030. zbl MR doi

[2] *G. Bao, L. Zhang*: Shape reconstruction of the multi-scale rough surface from multi-frequency phaseless data. Inverse Probl. *32* (2016), Article ID 085002, 16 pages. zbl MR doi

[3] *D. Colton, R. Kress*: Inverse Acoustic and Electromagnetic Scattering Theory. Applied Mathematical Sciences 93, Springer, New York, 2013. zbl MR doi

[4] *O. Ivanyshyn*: Shape reconstruction of acoustic obstacles from the modulus of the far field pattern. Inverse Probl. Imaging *1* (2007), 609–622. zbl MR doi

[5] *O. Ivanyshyn, T. Johansson*: Nonlinear integral equation methods for the reconstruction of an acoustically sound-soft obstacle. J. Integral Equations Appl. *19* (2007), 289–308. zbl MR doi

[6] *O. Ivanyshyn, R. Kress*: Inverse scattering for planar cracks via nonlinear integral equations. Math. Methods Appl. Sci. *31* (2008), 1221–1232. zbl MR doi

[7] *O. Ivanyshyn, R. Kress*: Identification of sound-soft 3D obstacles from phaseless data. Inverse Probl. Imaging *4* (2010), 131–149. zbl MR doi

[8] *T. Johansson, B. D. Sleeman*: Reconstruction of an acoustically sound-soft obstacle from one incident field and the far-field pattern. IMA J. Appl. Math. *72* (2007), 96–112. zbl MR doi

[9] *A. Karageorghis, B. T. Johansson, D. Lesnic*: The method of fundamental solutions for the identification of a sound-soft obstacle in inverse acoustic scattering. Appl. Numer. Math. *62* (2012), 1767–1780. zbl MR doi
[10] *A. Kirsch, S. Ritter*: A linear sampling method for inverse scattering from an open arc. Inverse Probl. *16* (2000), 89–105. zbl MR doi
[11] *R. Kress*: Fréchet differentiability of the far field operator for scattering from a crack. J. Inverse Ill-Posed Probl. *3* (1995), 305–313. zbl MR doi
[12] *R. Kress*: Inverse scattering from an open arc. Math. Methods Appl. Sci. *18* (1995), 267–293. zbl MR doi
[13] *R. Kress, W. Rundell*: Inverse obstacle scattering with modulus of the far field pattern as data. Inverse Problems in Medical Imaging and Nondestructive Testing (H. W. Engl et al., eds.). Springer, Wien, 1997, pp. 75–92. zbl MR doi
[14] *R. Kress, P. Serranho*: A hybrid method for two-dimensional crack reconstruction. Inverse Probl. *21* (2005), 773–784. zbl MR doi
[15] *K.-M. Lee*: Shape reconstructions from phaseless data. Eng. Anal. Bound. Elem. *71* (2016), 174–178. MR doi
[16] *X. Liu, B. Zhang*: Unique determination of a sound-soft ball by the modulus of a single far field datum. J. Math. Anal. Appl. *365* (2010), 619–624. zbl MR doi
[17] *L. Mönch*: On the inverse acoustic scattering problem by an open arc: the sound-hard case. Inverse Probl. *13* (1997), 1379–1392. zbl MR doi
[18] *Y. Yan, I. H. Sloan*: On integral equations of the first kind with logarithmic kernels. J. Integral Equations Appl. *1* (1988), 549–579. zbl MR doi

Authors' address: *Peng Gao*, *Heping Dong* (corresponding author), *Fuming Ma*, Institute of Mathematics, Jilin University, Changchun 130012, China, e-mail: penggao07@163.com, dongheping2001@sina.com, mfm@jlu.edu.cn.